Supporting Information

A microcrystalline soft carbon modified hard carbon coating enhances cycling stability and initial efficiency in natural graphite anodes

Jiangtao Liang[a], Pengtao Wang[a], Zhuoqi Liu[b], Song Yang[*a], Shoujun Liu[a], Junhao Liu[cd],Xuzhong Gong[*cd]

[a] College of chemistry and chemical engineering, Taiyuan University of Technology, 030024, Taiyuan, China. E-mail: liangjiangtao1009@163.com

[b] Shenzhen Guangfeng New Energy Technology Co., Ltd, Shenzhen, 518000, China

[c] College of Environmental and Chemical Engineering, Heilongjiang University of Science and Technology, Harbin, 150022, China

[d] College of Chemical Engineering, University of Chinese Academy of Sciences, Beijing, 100049, China. E-mail: xzgong@ipe.ac.cn

[*] Corresponding author: Song Yang, yangsong@tyut.edu.cn

Xuzhong Gong, xzgong@ipe.ac.cn

Prior to the double cladding treatment, we carried out deep purification of natural

graphite tails by a two-step method: Pretreatment stage: preliminary purification to 97.03% using hydrochloric acid at 60℃ (4h); Electrolytic purification stage: the pretreated graphite (4g) was pressed and further purified to 99.90% in HF-H_2SO_4 (3mL 40 wt.% and 5mL 0.5 M H_2SO_4 and 32mL H_2O)electrolyte system (4V, 30℃, platinum pairs of electrodes) with 96.00% yield. See Fig. S1 and S2 for purification process and data, respectively.

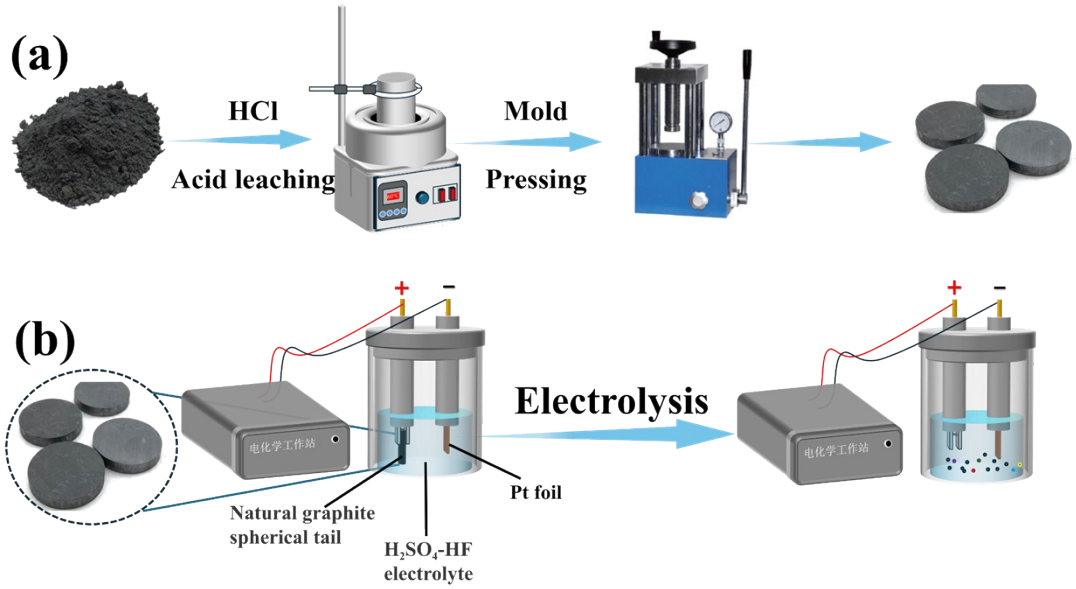

Fig. S1 Natural graphite purification flow chart.

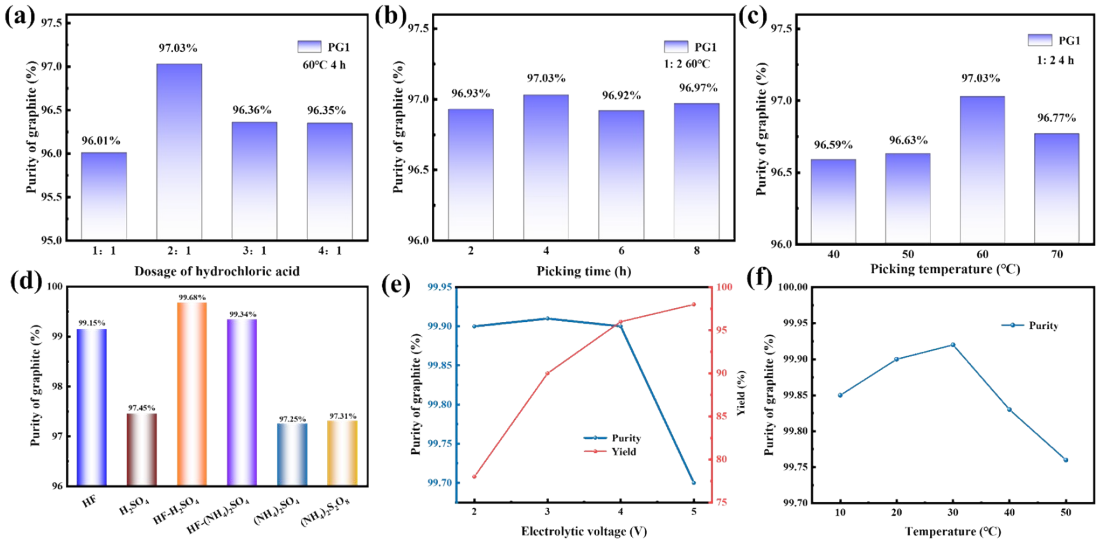

Fig. S2 Natural graphite ball end purification data.

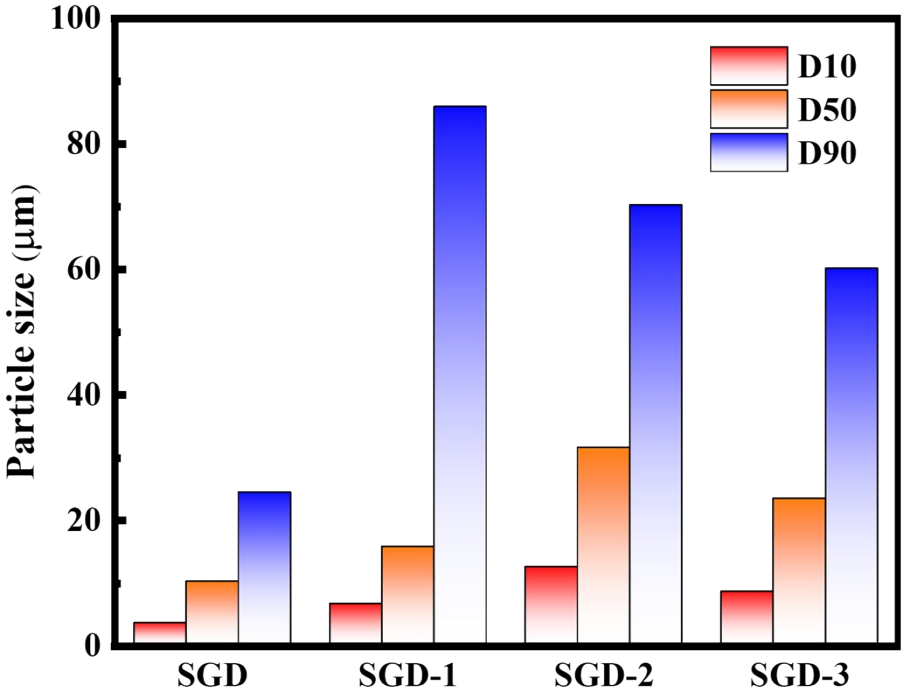

Fig. S3 Compare the particle size distribution of the sample.

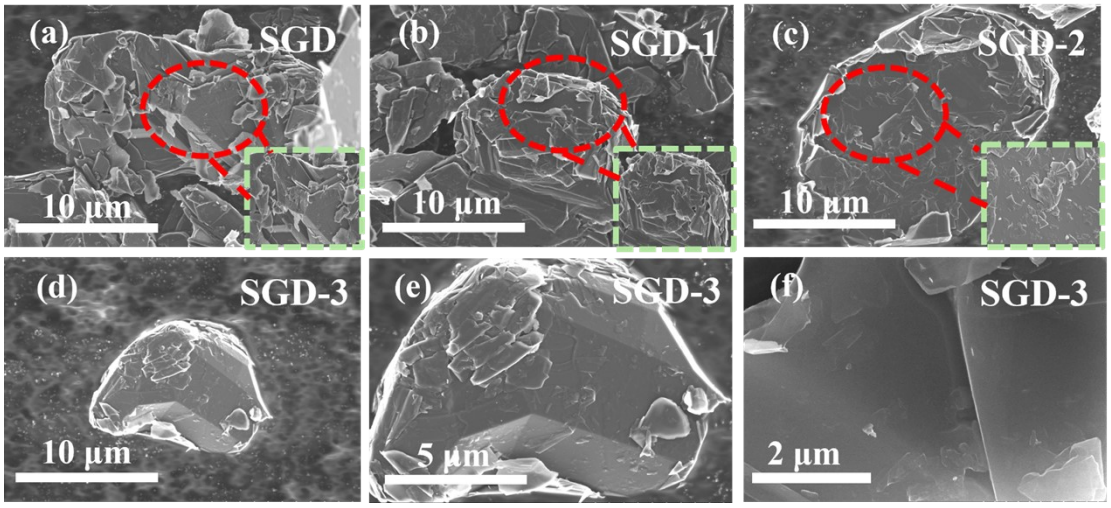

Fig. S4 SEM image of (a) SGD, (b) SGD-1, (c) SGT-2, (d-f) SGD-3.

Table S1 Specific surface area and pore volume distribution data of SGD、SGD-1、SGD-2 and SGD-3.

Sample	S_{BET} /（$m^2 \cdot g^{-1}$）	Pore volume/（$cm^3 \cdot g^{-1}$）
SGD	7.4319	0.038492
SGD-1	55.0337	0.024415
SGD-2	4.3521	0.016708
SGD-3	3.0638	0.009946

Table S2 Element content of each sample.

Sample	C(at.%)	O(at.%)
SGD	97.99	2.01
SGD-1	98.35	1.65
SGD-2	98.39	1.61
SGD-3	98.72	1.28

Table S3 C content of each sample.

Samples	C 1s	C-C/C=C	C-O	C=O	O-C=O
SGD	Peak value (eV)	284.60	286.80	287.70	290.70
	Content (%)	75.49	3.71	4.84	15.96
SGD-1	Peak value (eV)	284.60	286.30	287.30	290.60
	Content (%)	73.01	7.44	5.54	14.01
SGD-2	Peak value (eV)	284.61	286.90	287.90	291.40
	Content (%)	78.52	4.27	4.53	12.68
SGD-3	Peak value (eV)	284.60	286.40	287.50	291.10
	Content (%)	79.611	4.10	3.34	12.94

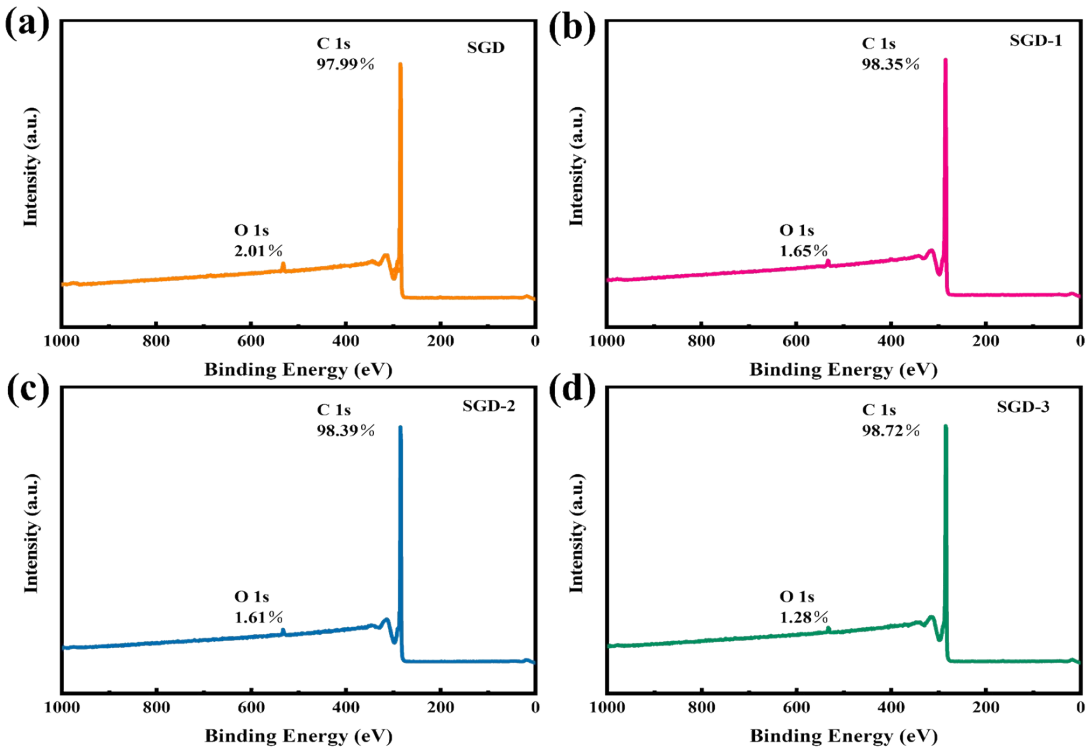

Fig. S5 X-ray photoelectron spectroscopy (XPS) analysis of (a) SGD, (b) SGD-1, (c) SGD-2 and (d) SGD 3.

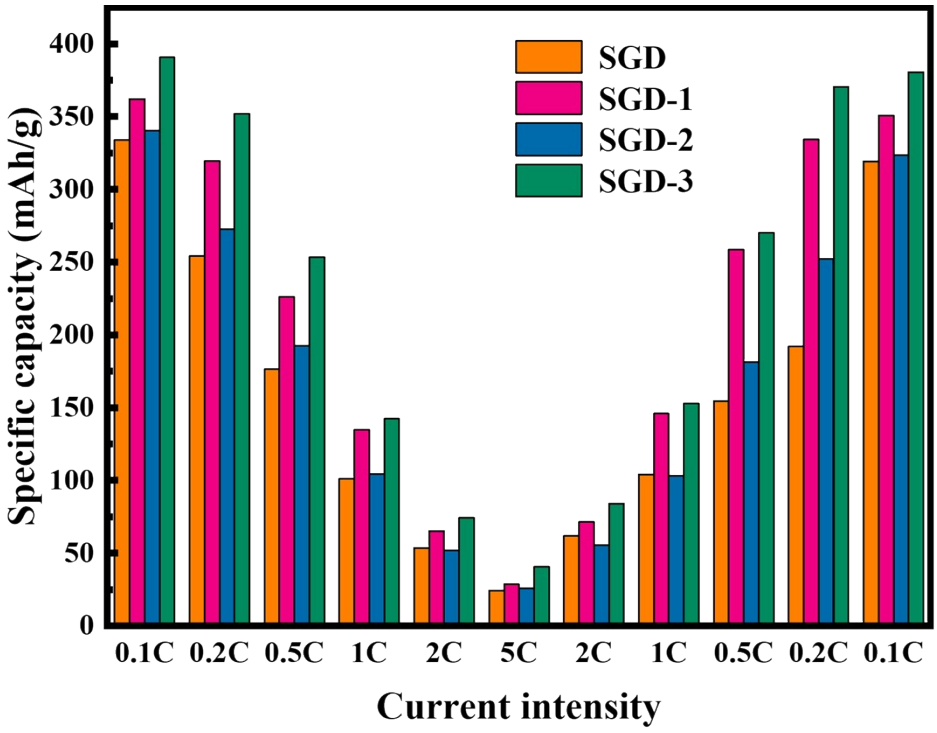

Fig. S6 Rate capacity of SGD, SGD-1, SGD-2 and SGD-3.

We mixed phenolic resin with bitumen in the ratio of 1:1, and subsequently carbonized natural graphite with phenolic resin and bitumen mixture in the ratio of 8:2 at 900 °C, holding time of 2 h, and a temperature increase rate of 5°/min, notated as SGD-1-3. Compared with one-step (8:2), the two-step method significantly improves the particle size by optimizing the structure of the carbon layers in stages size, vibrational density, interfacial stability, and electrochemical properties (Fig. S5). In terms of physical properties, the two-step method achieved a more homogeneous particle encapsulation with a reduction of about 4.1% in D50 (23.446 μm) compared to the one-step method (24. 458 μm), which was attributed to the porous skeleton formed by the first layer of phenolic resin in the step-by-step encapsulation process, which provided a uniform anchorage for the secondary encapsulation of the asphalt, and effectively avoided separation of the component phases during the hybrid encapsulation process. This structural optimization is further reflected in the increase of vibration density, which is 20.2% higher in the two-step method (1.01 g cm^{-3}) than that in the one-step method (0.84 g cm^{-3}), which indicates that the gradual construction of the structure of the "hard carbon skeleton - soft carbon filler" has resulted in a denser arrangement of particles. The specific surface area data (3.0638 $m^2 g^{-1}$ for the two-step method and 6.4068 $m^2 g^{-1}$ for the one-step method) confirmed that the two-step method resulted in a better integrity of the carbon layer and less pore exposure, which laid the foundation for the subsequent improvement of the electrochemical performance.

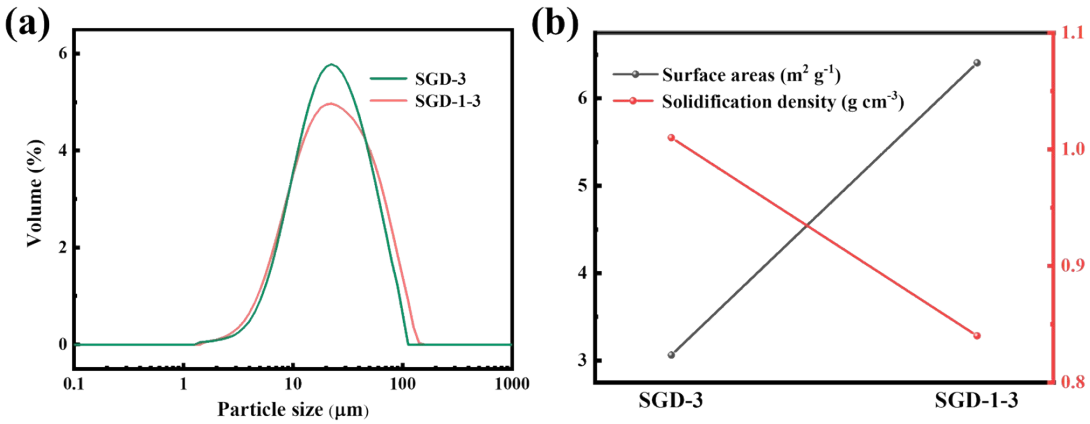

Fig. S7 Particle size distribution of SGD-3 and SGD-1-3 (a); (b) Specific surface vs. vibration density of SGD-3 and SGD-1-3.

In terms of electrochemical performance, the advantage of the two-step method is more prominent (Fig. S6). The first efficiency is increased from 77.81% to 85.79% in the one-step method, which is attributed to the low specific surface area carbon layer

effectively inhibiting the irreversible decomposition of the electrolyte on the graphite surface. The cycling stability test shows that the capacity of the two-step method remains 344.10 mAh g^{-1} (92% retention rate) after 80 cycles at 0.1 C, which is significantly better than that of the one-step method at 316.5 mAh g^{-1} (85% retention rate), and this difference is mainly attributed to the formation of a uniform and dense carbon layer in the two-step method: on the one hand, the hard carbon skeleton derived from phenol-formaldehyde resin mitigates the volumetric expansion of the graphite, and on the other hand, the bitumen filled soft carbon layer provides a stable ion transport channel. Taken together, the two-step method successfully solves the problems of uneven component distribution and pore defects caused by simultaneous carbonization in the one-step method by accurately controlling the carbon layer structure in stages.

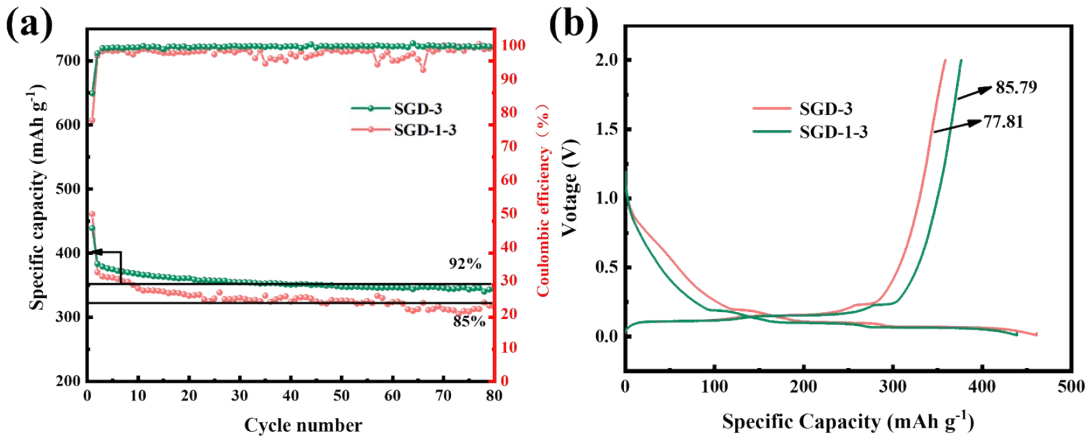

Fig. S8 The cycling performance of SGD-3 and SGD-1-3 at 0.1C is demonstrated (a); (b) initial constant current charge/discharge curves.